Title

Chemical Differences between Phenolic Secondary Organic Aerosol Formed through Gas-Phase and Aqueous-Phase Reactions

Journal

ACS Earth and Space Chemistry, 8(11)

ISSN

2472-3452

Authors

Jiang, Wenqing

Yu, Lu

Yee, Lindsay

et al.

Publication Date

2024-11-21

DOI

10.1021/acsearthspacechem.4c00204

Peer reviewed

ACS EARTH AND SPACE CHEMISTRY

http://pubs.acs.org/journal/aesccq
Article

Chemical Differences between Phenolic Secondary Organic Aerosol Formed through Gas-Phase and Aqueous-Phase Reactions

Published as part of ACS Earth and Space Chemistry special issue "Hartmut Hermann Festschrift".

Wenqing Jiang, Lu Yu, Lindsay Yee, Puneet Chhabra, John Seinfeld, Cort Anastasio, and Qi Zhang*

Cite This: *ACS Earth Space Chem.* 2024, 8, 2270−2283

Read Online

ACCESS | Metrics & More | Article Recommendations | Supporting Information

ABSTRACT: Phenolic compounds, which are significant emissions from biomass burning (BB), undergo rapid photochemical reactions in both gas and aqueous phases to form secondary organic aerosol, namely, gasSOA and aqSOA, respectively. The formation of gasSOA and aqSOA involves different reaction mechanisms, leading to different product distributions. In this study, we investigate the gaseous and aqueous reactions of guaiacol—a representative BB phenol—to elucidate the compositional differences between phenolic aqSOA and gasSOA. Aqueous-phase reactions of guaiacol produce higher SOA yields than gas-phase reactions (e.g., roughly 60 vs 30% at one half-life of guaiacol). These aqueous reactions involve more complex reaction mechanisms and exhibit a more gradual SOA evolution than their gaseous counterparts. Initially, gasSOA forms with high oxidation levels (O/C > 0.82), while aqSOA starts with lower O/C (0.55−0.75). However, prolonged aqueous-phase reactions substantially increase the oxidation state of aqSOA, making its bulk chemical composition closer to that of gasSOA. Additionally, aqueous reactions form a greater abundance of oligomers and high-molecular-weight compounds, alongside a more sustained production of carboxylic acids. AMS spectral signatures representative of phenolic gasSOA have been identified, which, together with tracer ions of aqSOA, can aid in the interpretation of field observation data on aerosol aging within BB smoke. The notable chemical differences between phenolic gasSOA and aqSOA highlighted in this study also underscore the importance of accurately representing both pathways in atmospheric models to better predict the aerosol properties and their environmental impacts.

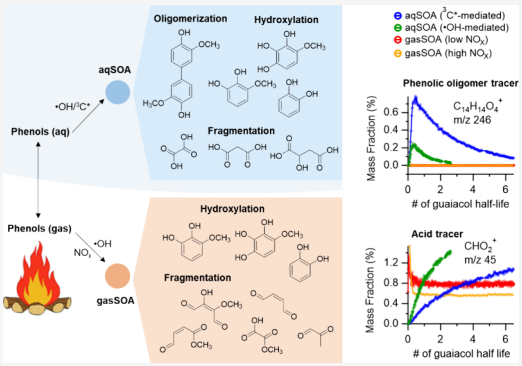

KEYWORDS: *secondary organic aerosols, phenols, gas-phase photoreactions, aqueous-phase photoreactions, oligomerization, acid formation, guaiacol, biomass burning*

1. INTRODUCTION

Secondary organic aerosol (SOA) makes up a significant fraction of tropospheric aerosol mass,[1,2] playing crucial roles in affecting human health, air quality, and climate.[3,4] Due to a multitude of emission sources and the intricate interplay of physical and chemical processes in the atmosphere, the chemical composition of SOA is extremely complex. Traditionally, SOA formation has been attributed to gas-phase oxidation of volatile organic compounds (VOCs), followed by the partitioning of low-volatility products into the particle phase. However, an increasing body of research indicates that atmospheric liquid water (e.g., cloud and fog droplets and particle water) can facilitate the partitioning of water-soluble VOCs and semivolatile organic compounds (SVOCs) into the aqueous phase, where they can undergo reactions to form low-volatility SOA species.[5−8] Aqueous-phase reactions can occur on similar or even shorter time scales compared to gas-phase reactions. For example, the lifetimes of phenols with respect to gas-phase hydroxyl radical (•OH) reactions are typically on the order of hours,[9] while the lifetimes of phenols with respect to aqueous-phase •OH reactions range from minutes to hours.[10] Moreover, the pseudo-first-order reaction rates of phenols with other aqueous-phase oxidants, such as the excited state of organic carbon ($^3C^*$) and singlet oxygen ($^1O_2$), can be comparable or higher than those with •OH in the aqueous phase.[10−13] Considering the prevalence of cloud, fog, and aerosol water, along with the fast formation rates and significant yields of SOA resulting from aqueous reactions of various water-soluble VOCs and SVOCs (e.g., aldehydes, phenols, and glyoxal),[13−16] it is estimated that the mass of SOA formed through aqueous-phase reactions (aqSOA) is

Received: July 13, 2024
Revised: September 3, 2024
Accepted: October 2, 2024
Published: October 10, 2024

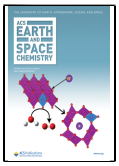

comparable to that formed through gas-phase reactions (gasSOA) in the atmosphere.[17,18]

AqSOA also significantly influences the composition and properties of aerosols. Compared to gasSOA, aqSOA generally consists of molecules with substantially different distributions of molecular weight, oxygen-to-carbon (O/C) ratio, functional groups, viscosity, and optical and water-uptake properties.[19−23] The elevated oxygenation of aqSOA, which is in part due to the high O/C ratios found in common aqSOA precursors, such as glyoxal and methylglyoxal,[17] can enhance its hygroscopicity and ability to nucleate cloud droplets, influencing cloud formation. However, this characteristic also makes aqSOA more susceptible to wet deposition, resulting in a shorter atmospheric lifetime.[24,25] Additionally, aqueous reactions can generate light-absorbing species, making them a significant source of brown carbon aerosol.[26,27]

Phenols represent an important family of aromatic volatile and semivolatile compounds released through lignin pyrolysis during biomass burning (BB).[28] Apart from participating in gas-phase reactions that contribute to SOA formation,[29−31] phenols possess high Henry's law constants (K_H)[32] and react rapidly with aqueous-phase oxidants, such as hydroxyl radical (•OH), singlet oxygen ($^1O_2$*), and triplet excited states of organics (^{3}C*), forming aqSOA with high mass yields.[10,12,15,33] The relative contributions of phenolic gasSOA and aqSOA under ambient conditions depend on factors, such as the K_H of phenols, liquid water content, and oxidant concentrations.[12,34] Model simulations suggest that in highly humid environments, aqSOA could dominate overall SOA formation from phenols.[13] Furthermore, recent ambient measurements suggest that the formation rate of phenolic aqSOA can surpass that of phenolic gasSOA under foggy conditions.[35]

Guaiacol (2-methoxyphenol, GUA) is a VOC emitted from both hardwood and softwood burning.[36] Under low-NO_x conditions, guaiacol produces SOA through gas-phase •OH photooxidation, with average mass yields in the range of 44−50%.[29] The gas-phase reaction initiates with either H-abstraction from the hydroxyl group, resulting in the formation of a phenoxy radical, or •OH addition to the aromatic ring, leading to the generation of an organic peroxy radical. Subsequent reactions involve hydroxylation, isomerization, epoxide formation, fragmentation (ring-opening reactions), and/or loss of a methoxy group.[29] Under high NO_x conditions, nitrophenols are formed.[29,37]

Guaiacol is highly effective in generating aqueous SOA as well. It exhibits moderate partitioning to atmospheric waters (K_H = 8.7 × 10^2 M atm^{-1})[32] and undergoes aqueous-phase reactions with •OH and ^{3}C* that lead to the production of aqSOA with mass yields close to 100%.[10,38,39] Key reactions involved in this process include oligomerization, functionalization, esterification, demethoxylation, and fragmentation.[38−40] Despite the crucial role of aqueous-phase reactions, current models often overlook the formation of aqSOA from BB-emitted phenols. This oversight can lead to underestimating the impact of BB on the SOA budget and its effects on the climate. Additionally, due to differences in mass yields, composition, and optical properties, it is essential to distinguish between phenolic gasSOA and aqSOA to accurately represent BB SOA when evaluating air quality and climate impacts.

In the present study, we compare the chemical composition and evolution dynamics of guaiacol gasSOA and aqSOA formation, drawing on previous laboratory results. We contrast measurements of SOA using Aerodyne high-resolution time-of-flight aerosol mass spectrometers (HR-ToF-AMS), with a specific emphasis on identifying chemical distinctions between guaiacol gasSOA and aqSOA, particularly regarding key products, such as oligomers and carboxylic acids. We explore potential factors that may contribute to the different formation mechanisms of guaiacol gasSOA and aqSOA. Through this comparative analysis, our goal is to gain insights into the product distributions and chemical transformations occurring in guaiacol's gas-phase and aqueous-phase photoreactions. These insights may contribute to a more comprehensive understanding of SOA formation from phenolic precursors, particularly within the context of BB emissions.

2. EXPERIMENTAL METHODS

2.1. Photooxidation Experiments. A summary of the gas-phase and aqueous-phase photochemical oxidation experiments of guaiacol ($C_7H_8O_2$) is presented in Table S1 in the Supporting Information. Briefly, aqueous-phase photoreaction experiments were performed within an RPR-200 photoreactor equipped with bulbs of three different types (300, 350, and 419 nm) to roughly simulate sunlight,[41] which entailed the reactions of guaiacol with •OH or ^{3}C* following the procedures outlined by Yu et al.[38,40] In these experiments, 100 μM guaiacol was dissolved in air-saturated Milli-Q water and adjusted to pH 5 using sulfuric acid. For •OH experiments, 100 μM H_2O_2 was introduced into the initial solution as the source of •OH. In the ^{3}C* experiments, 5 μM 3,4-dimethoxybenzaldehyde (3,4-DMB) was added to the solution as the source of ^{3}C*.

Gas-phase experiments were conducted in Caltech's dual 28 m^3 Teflon laboratory chambers, under either low-NO_x or high-NO_x conditions, involving the photochemical reactions of guaiacol with •OH, as described by Yee et al.[29] In the low-NO_x experiments (initial NO_x concentration <5 ppb), the initial guaiacol concentration was 5.9 ppb, with H_2O_2 serving as the •OH source. In the high-NO_x experiments (initial NO_x concentration reached hundreds of ppb), the initial guaiacol concentration was 55.3 ppb, with HONO used as the •OH source. These chamber experiments were conducted under dry conditions with RH maintained below 10%. Ammonium sulfate seed aerosol was used to facilitate the condensation of the oxidation products. Illumination (340−350 nm) was from three hundred 40 W black lights.[29]

The phenolic precursor concentrations used in the photochemical reactions are representative of the atmospheric conditions influenced by BB. Previous studies have shown that the atmospheric gas-phase concentrations of phenols can vary from 0.03 to 44 ppb,[42] while the aqueous-phase concentrations of phenols in cloud and fog waters typically range from 0.1 to 30 μM.[43] In regions impacted by BB, the aqueous-phase concentrations of phenols have been predicted to exceed 100 μM.[43]

2.2. HR-ToF-AMS Data Analysis. High-resolution time-of-flight aerosol mass spectrometers (Aerodyne Research Inc., Billerica, MA) were used to characterize the chemical composition of both gasSOA and aqSOA, including average elemental ratios, such as the atomic oxygen-to-carbon ratio (O/C), hydrogen-to-carbon ratio (H/C), and fragment ions. For gasSOA, the signals of CO^+ and the H_2O-related ions (e.g., H_2O^+, HO^+, and O^+) were estimated using the method described by Aiken et al.[44] For aqSOA, since argon was used for atomization and the resulting aerosols were thoroughly

https://doi.org/10.1021/acsearthspacechem.4c00204
ACS Earth Space Chem. 2024, 8, 2270−2283

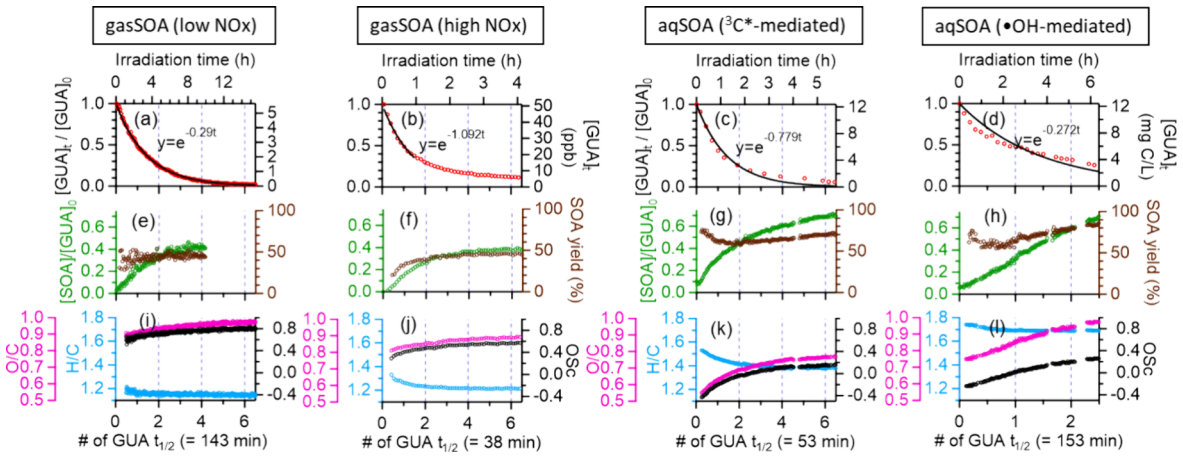

Figure 1. Gas-phase and aqueous-phase reaction kinetics of guaiacol and the chemical evolution of the resulting SOA as a function of the number of guaiacol half-lives elapsed (bottom horizontal axis) and irradiation time (top horizontal axis). (a–d) Decay of guaiacol, (e–h) SOA mass yields, and (i–l) H/C, O/C, and OSc of the guaiacol SOA. The fitting equations in panels (a–d) show the exponential decay of guaiacol as a function of irradiation time (t).

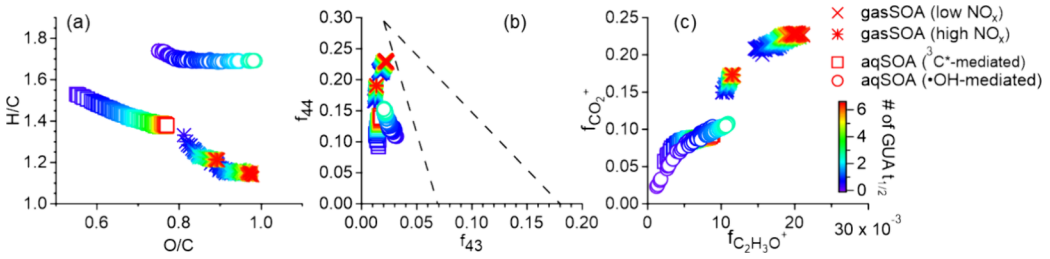

Figure 2. Evolution of guaiacol gasSOA and aqSOA depicted in (a) Van Krevelen diagram, (b) f_{44} vs f_{43} space, and (c) f_{CO2+} vs f_{C2H3O+} space based on AMS measurements. The dashed lines in panel (b) denote the boundaries for oxygenated organic aerosols (OOAs) observed in ambient environments.[75] In this study, $C_2H_3O^+$ consistently contributes a dominant fraction (91–100%) of m/z 43 in gasSOA, with $C_3H_7^+$ accounting for only a minor portion. In contrast, the contribution of $C_2H_3O^+$ to m/z 43 in aqSOA increases from 29 to 80% as photooxidation progresses, which results in different trends of f_{43} and f_{C2H3O+} in aqSOA.

dried, CO^+ and the H_2O-related ions were determined directly in the spectra of aqSOA.[38] The average oxidation state of carbon (OSc), indicating the oxidation degree of SOA, was calculated using the formula $OS_C = 2 \times O/C - H/C$, as described by Kroll et al.[45]

Positive matrix factorization (PMF) analysis was performed on the AMS mass spectral matrix, along with the corresponding error matrix generated within PIKA. The PMF results were evaluated using the PMF Evaluation Toolkit (PET v3.08), following the established criteria.[46,47] A two-factor solution was determined to be suitable for gasSOA formed under both low-NO_x and high-NO_x conditions. For aqSOA, a three-factor solution was chosen for $^3C^*$-initiated reactions, while a four-factor solution, consisting of three distinct aqSOA factors and one background factor, was used for •OH-initiated reactions. Selecting fewer or more factors led to either elevated residuals or factor splitting. Detailed information regarding the PMF analysis for each experiment is given in the Supporting Information (S1).

3. RESULTS AND DISCUSSION

3.1. Different Formation Kinetics and Chemical Evolution Profiles of Guaiacol AqSOA and GasSOA.

Figure 1 provides an overview of the kinetics and illustrates the changes in the bulk chemical properties of the resulting SOA during the photoreactions of guaiacol in both the gas and aqueous phases. To facilitate comparisons across different experiments, these changes are presented relative to the number of half-lives ($t_{1/2}$) of guaiacol decay. While both guaiacol gasSOA and aqSOA become more oxidized over the course of the photoreactions, there are notable differences in their initial oxidation states and the rate of oxidation during experiments. As shown in Figure 1i–l, gasSOA starts with a higher degree of oxidation compared to aqSOA, but the increase in oxidation is more pronounced for aqSOA as the photoreactions progress. For example, the O/C ratio of aqSOA resulting from the $^3C^*$-mediated reaction increases by 0.22 from the beginning of the reaction to six half-lives of guaiacol (Figure 1k), while those of gasSOA from both low- and high-NO_x conditions only increase by around 0.07 (Figure 1i,j). The •OH-mediated photooxidation of guaiacol was run for 2.6 half-lives, during which the O/C of aqSOA increases by 0.23 (Figure 1l). These observations indicate that the oxidation states of gasSOA and aqSOA evolve differently during their photoreactions and that the aqueous-phase reactions tend to produce SOA with a broader range of oxidation states.

The higher degree of oxidation in gasSOA compared with aqSOA during the initial stages of photochemical reactions can be partially attributed to the higher availability of oxidants in gas-phase reactions. As shown in Table S1, the estimated •OH concentrations in the gas-phase reactions are in the range of $(1.1–4.5) \times 10^6$ molecules cm^{-3}, leading to an initial oxidant-to-guaiacol molar ratio of $(3.5–7.8) \times 10^{-6}$. However, in aqueous-phase reactions, the initial oxidant-to-guaiacol molar

https://doi.org/10.1021/acsearthspacechem.4c00204
ACS Earth Space Chem. 2024, 8, 2270–2283

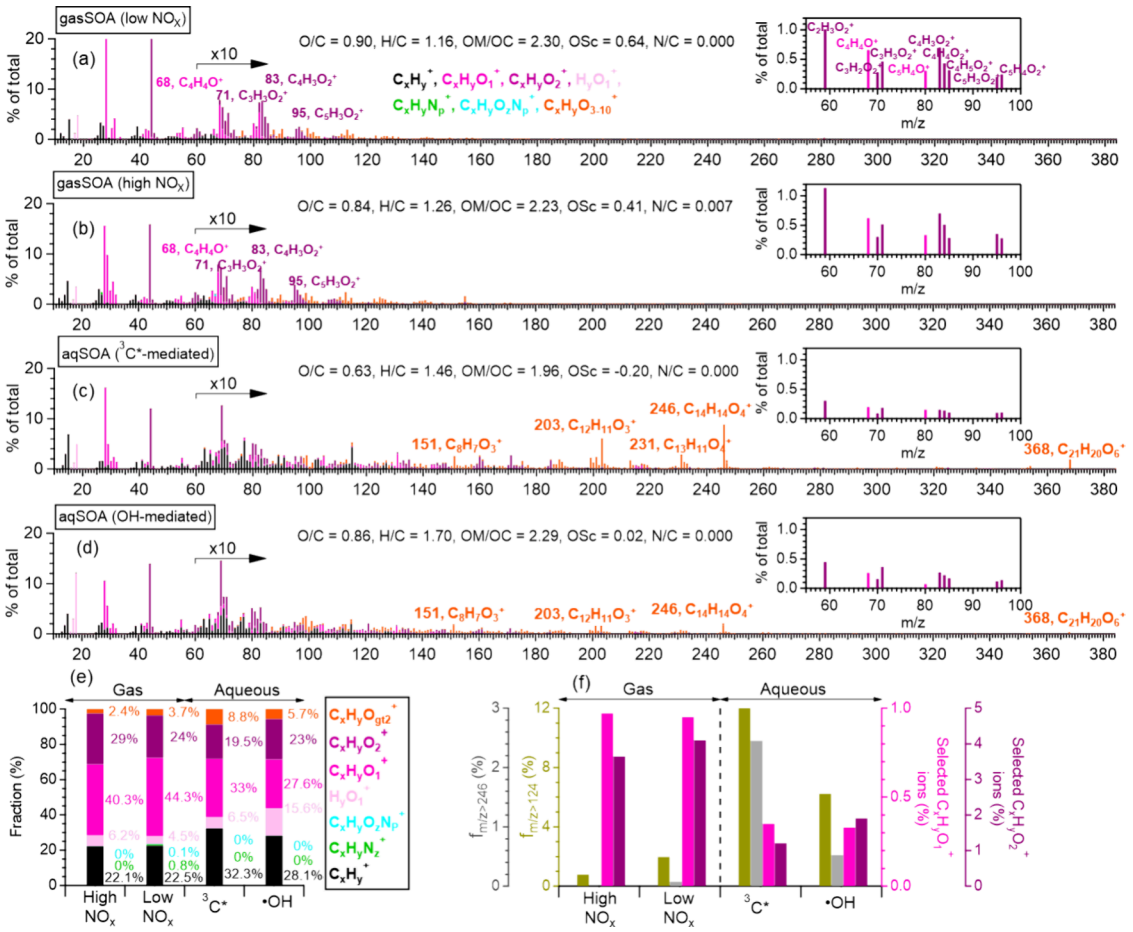

Figure 3. AMS spectra of (a,b) gasSOA and (c,d) aqSOA formed at one half-life ($t_{1/2}$) of guaiacol. The insets highlight a group of $C_xH_yO_1^+$ and $C_xH_yO_2^+$ ions in m/z 59−96 that are more enhanced in gasSOA compared to aqSOA. Mass fractions of (e) different ion categories and (f) large ions ($f_{m/z>124}$ and $f_{m/z>246}$), the sum of selected $C_xH_yO_1^+$ ions (e.g., $C_4H_4O^+$ and $C_5H_4O^+$), and the sum of selected $C_xH_yO_2^+$ ions ($C_2H_3O_2^+$, $C_3H_2O_2^+$, $C_3H_3O_2^+$, $C_4H_3O_2^+$, $C_4H_4O_2^+$, $C_4H_5O_2^+$, $C_5H_3O_2^+$, $C_5H_4O_2^+$) in the AMS spectra of gasSOA and aqSOA at $t_{1/2}$ of guaiacol.

ratio is considerably lower in the range of $(0.48-8.8) \times 10^{-10}$. The greater oxidant availability in gas-phase reactions likely creates a highly oxidative environment for guaiacol molecules, prompting the rapid formation of highly oxidized products.

The chemical differences between aqSOA and gasSOA appear to be more pronounced when they are freshly formed. The difference gradually decreases as the photoreactions progress, suggesting a convergence in the chemical composition of guaiacol SOA resulting from further oxidation and fragmentation in the two phases. In Figure 2, we use the Van Krevelen diagram and scatter plots of f_{44} vs f_{43} and f_{CO2+} vs f_{C2H3O+} to compare the evolution trends in the bulk chemical properties of guaiacol gasSOA and aqSOA during photoreactions. The shifts in H/C and O/C ratios depicted in the Van Krevelen diagram provide insights into the transformation mechanism of OA during the given experiment.[48] For example, a slope of −2 likely suggests the replacement of an aliphatic carbon with a carbonyl group. A slope of 0 implies an increase in the oxygen content with no change in hydrogen, potentially resulting from replacing a hydrogen atom with an alcohol or a peroxide group. A slope of −1, which is common as OA aging progresses,[48] denotes the simultaneous addition of both functional groups, forming a hydroxycarbonyl or carboxylic acid. In this study, the slopes of guaiacol gasSOA tend to be closer to −1, while those of aqSOA are closer to 0. This distinction implies that the dominant reaction mechanisms of guaiacol may differ between the gas phase and the aqueous phase.

In the plots of f_{44} vs f_{43} and f_{CO2+} vs f_{C2H3O+}, gasSOA initially shows considerably higher f_{44} and f_{CO2+} values than aqSOA, indicating a higher degree of oxidation and acid formation of gasSOA at the beginning of the photoreactions. However, as the photoreactions progress, f_{CO2+} of aqSOA increases significantly, whereas f_{CO2+} of gasSOA shows only a minimal increase. This observation suggests that aqSOA becomes increasingly oxidized over time due to photochemical reactions in the aqueous phase, while gasSOA maintains a relatively high degree of oxidation throughout its gas-phase reactions. However, it is important to note that the oxidation degree of gasSOA reflects a complex interplay between gas-phase oxidative aging and the increased partitioning of less volatile species into the particle phase as SOA loading increases.

In line with the more pronounced bulk chemical evolution observed in aqueous-phase reactions, the growth in the SOA mass during prolonged aqueous-phase reactions is more significant than that in gas-phase reactions. Under both low-NO_x and high-NO_x conditions, the gasSOA mass concentrations plateau at approximately two half-lives of guaiacol (Figure 1e,f) whereas the aqSOA concentrations continue to increase over the duration of the $^3C^*$- and •OH-mediated reactions, which last for 2.6 and 6.5 guaiacol half-lives, respectively (Figure 1g,h). The average mass yield of gasSOA

https://doi.org/10.1021/acsearthspacechem.4c00204
ACS Earth Space Chem. 2024, 8, 2270−2283

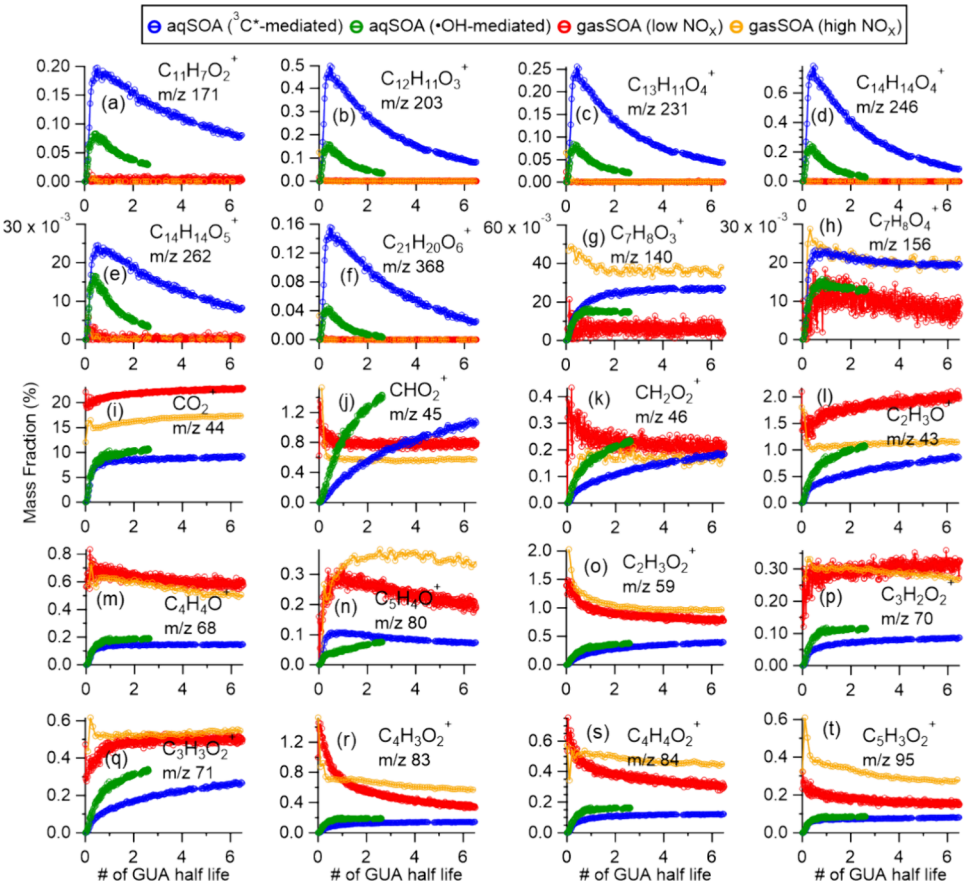

Figure 4. Mass fraction (% of total organic signal) of AMS tracer ions for guaiacol SOA over the course of the gas- and aqueous-phase reactions, including (a–f) oligomer-related ions, (g,h) hydroxylated guaiacol ions, (i–k) acid ions, and (l–t) $C_xH_yO_1^+$ and $C_xH_yO_2^+$ ions.

is significantly lower compared to that of aqSOA (~44 vs ~70%). This fact, along with the more sustained mass growth of aqSOA, suggests that the aqueous-phase reactions of guaiacol are more efficient at generating low-volatility species compared to gas-phase reactions.

One possible explanation for the observed differences in formation kinetics between aqSOA and gasSOA lies in their distinct reaction environments. While aqSOA forms directly within the condensed phase, gasSOA formation involves the gas-phase oxidation of the precursor, followed by the partitioning of the resulting products into particles. The yield of gasSOA may be influenced by various factors, including the amount and volatility of the products, as well as the pre-existing aerosol mass onto which these products condense.[49] For example, a lower total aerosol mass concentration in the chamber may lead to a reduced yield of guaiacol gasSOA. Additionally, the initial concentration of guaiacol strongly influences the mass yield of gasSOA, as demonstrated by Lauraguais et al., where higher initial guaiacol concentrations result in higher yield.[37] Moreover, SOA loading and the partitioning of gas-phase oxidation products can impact the composition of gasSOA. Previous studies have shown that under low SOA loadings, more oxygenated species tend to dominate, while higher SOA loadings promote the partitioning of more volatile and less oxygenated species into the particle phase, leading to a different SOA composition compared to conditions with low SOA mass loadings.[50]

3.2. Compositional Differences between Guaiacol AqSOA and GasSOA. Figure 3 compares the AMS spectra of guaiacol gasSOA and aqSOA obtained at one half-life of guaiacol, which represents the point when 50% of the initial guaiacol has reacted. The comparison reveals significant chemical disparities that highlight distinct pathways driving SOA formation between the aqueous phase and the gas phase. Specifically, the aqSOA spectra comprise a higher mass fraction of $C_xH_y^+$ ions but a lower fraction of $C_xH_yO_1^+$ ions compared to the gasSOA spectra (Figure 3e), indicating lower oxidation levels of the initially formed aqSOA species. Notably, the gasSOA spectra are missing common hydrocarbon ions with formulas $C_nH_{2n\pm1}^+$ ($n > 0$), such as $C_3H_5^+$, $C_3H_7^+$, $C_4H_7^+$, and $C_4H_9^+$ (Figure 3a–d). Furthermore, the characteristic fragment ions of the phenyl group (e.g., $C_6H_6^+$, $C_6H_5^+$, and $C_6H_4^+$) show substantially higher mass fractions in the spectra of aqSOA compared to gasSOA. This observation suggests that gas-phase photochemical reactions lead to a more significant loss or modification of the phenolic hydrocarbon structure compared to reactions occurring in the aqueous phase.

Further evidence supporting more fragmentation reactions in the gas phase compared with the aqueous phase comes from differences in the relative abundance of high m/z ions in their SOA mass spectra. As shown in Figure 3f, the mass fractions of ions heavier than 124 amu ($f_{m/z>124}$), i.e., larger than the molecular ion of guaiacol, are considerably greater in the guaiacol aqSOA spectra. Additionally, those heavier than 246 amu (i.e., m/z of guaiacol dimer) are completely absent in the gasSOA spectra but are present in the aqSOA spectra, especially with triplet oxidation. Since electron impact (EI) ionization produces ions up to the size of the molecular ion,

https://doi.org/10.1021/acsearthspacechem.4c00204
ACS Earth Space Chem. 2024, 8, 2270–2283

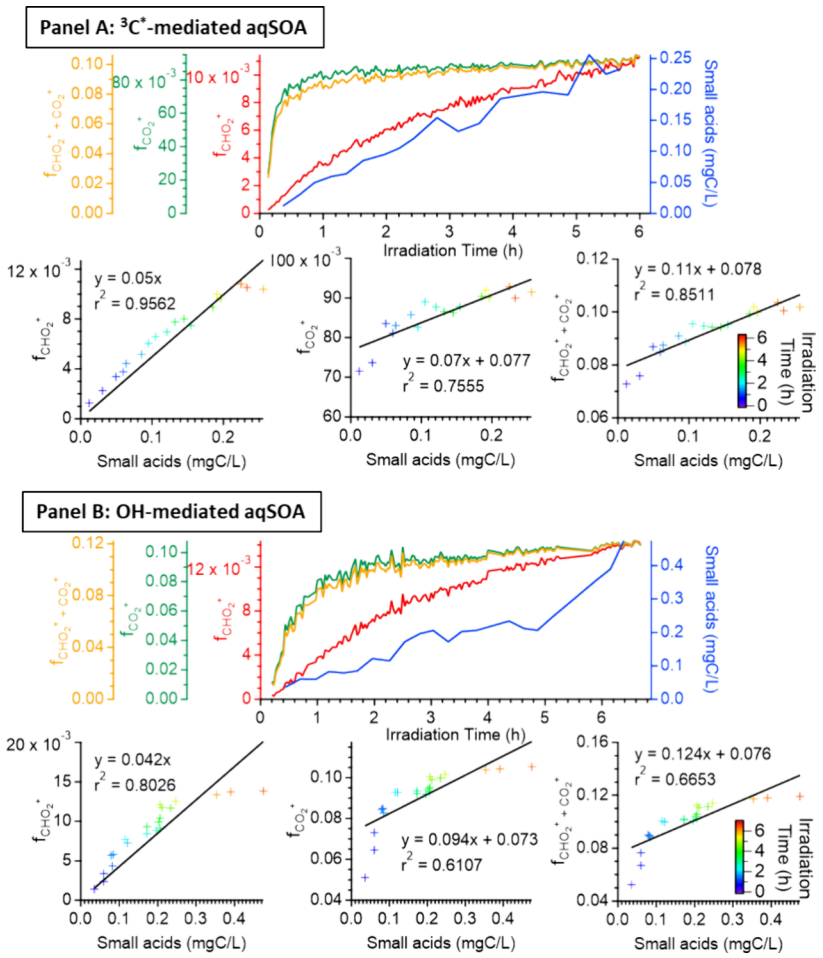

Figure 5. Time series of the AMS-measured f_{CHO2+}, f_{CO2+}, and $f_{(CHO2^{+}+CO2^{+})}$ and the total concentration of eight small organic acids (formic acid, acetic acid, pyruvic acid, malic acid, oxalic acid, malonic acid, fumaric acid, and maleic acid) measured by ion chromatography in guaiacol aqSOA and the correlations between these values in $^{3}C^{*}$-mediated (panel A) and OH-mediated (panel B) aqueous-phase reactions.

this indicates a higher occurrence of low-volatility, high-molecular-weight products in aqSOA compared to gasSOA.

A majority of high m/z ions in the aqSOA spectra are found to contain more than 2 oxygen atoms, prominently including those representing guaiacol oligomers (e.g., $C_{12}H_{11}O_3^+$, $C_{14}H_{14}O_4^+$, and $C_{21}H_{20}O_6^+$).[38] Previous studies showed that aqueous-phase photooxidation of phenols can swiftly produce dimers and higher oligomers through C−C or C−O coupling of phenoxy radicals (Scheme S1).[38,39,51] Furthermore, Braga et al. synthesized guaiacol dimers and identified m/z values of 246, 231, and 203 as the major fragment ions of guaiacol C−C dimer, while m/z values of 108 and 137 are prominent fragment ions of the guaiacol C−O dimer in 70 V EI mass spectra.[52] Our observations confirm the presence of peaks at m/z values of 246 ($C_{14}H_{14}O_4^+$), 231 ($C_{13}H_{11}O_4^+$), and 203 ($C_{12}H_{11}O_3^+$) in the guaiacol aqSOA spectra, with no significant signals appearing at m/z values of 108 and 137 (Figure 3c,d). Thus, it seems that C−C coupling, rather than C−O coupling, serves as the main mechanism for oligomerization in guaiacol aqSOA formation.

While the gasSOA spectra lack high m/z ions, they feature a distinct cluster of oxygenated ions in the m/z range of 59−96 amu (e.g., $C_2H_3O_2^+$, $C_3H_2O_2^+$, $C_3H_3O_2^+$, $C_4H_3O_2^+$, $C_4H_4O_2^+$, $C_4H_5O_2^+$, and $C_5H_3O_2^+$), which are in lesser prominence in the aqSOA spectra (Figures 3a,b,f and 4k−r). These $C_xH_yO_2^+$ ions can be derived from the fragmentation of esters and/or carboxylic acids in EI-MS.[53] For instance, $C_2H_3O_2^+$ can be generated from the breakdown of molecules containing CH_3O-CO- or $-CO-OCH_2-$ groups.[53] The elevated signals of the $C_xH_yO_2^+$ ions in the gasSOA spectra at one half-life of guaiacol may suggest a greater prevalence of esterification in the formation of gasSOA compared to aqSOA during the initial stage of reactions.

3.3. Contrasting the Chemical Evolution of AqSOA and GasSOA in Guaiacol Photoreactions. The comparisons of mass spectra discussed in the preceding section highlight a notable distinction between the aqueous-phase and gas-phase photooxidation of phenols: the formation of larger and more complex molecules is greatly favored through aqueous-phase reactions. To further examine the chemical evolutions of these components, Figure 4a−f depicts the temporal evolution of AMS tracer ions representing guaiacol oligomers (e.g., $C_{11}H_7O_2^+$, $C_{12}H_{11}O_3^+$, $C_{13}H_{11}O_4^+$, $C_{14}H_{14}O_4^+$, $C_{14}H_{14}O_5^+$, and $C_{21}H_{20}O_6^+$),[38] all of which exhibit noticeable increases at the beginning of the aqueous-phase reactions, followed by a decrease in the later periods. This pattern suggests that oligomers are generated during the initial phases of the aqueous-phase reactions but subsequently undergo decomposition and transformation into smaller molecules as the reactions progress. This is consistent with our previous findings, indicating that oligomerization primarily influences the initial generation of phenolic aqSOA, whereas functional-

https://doi.org/10.1021/acsearthspacechem.4c00204
ACS Earth Space Chem. 2024, 8, 2270−2283

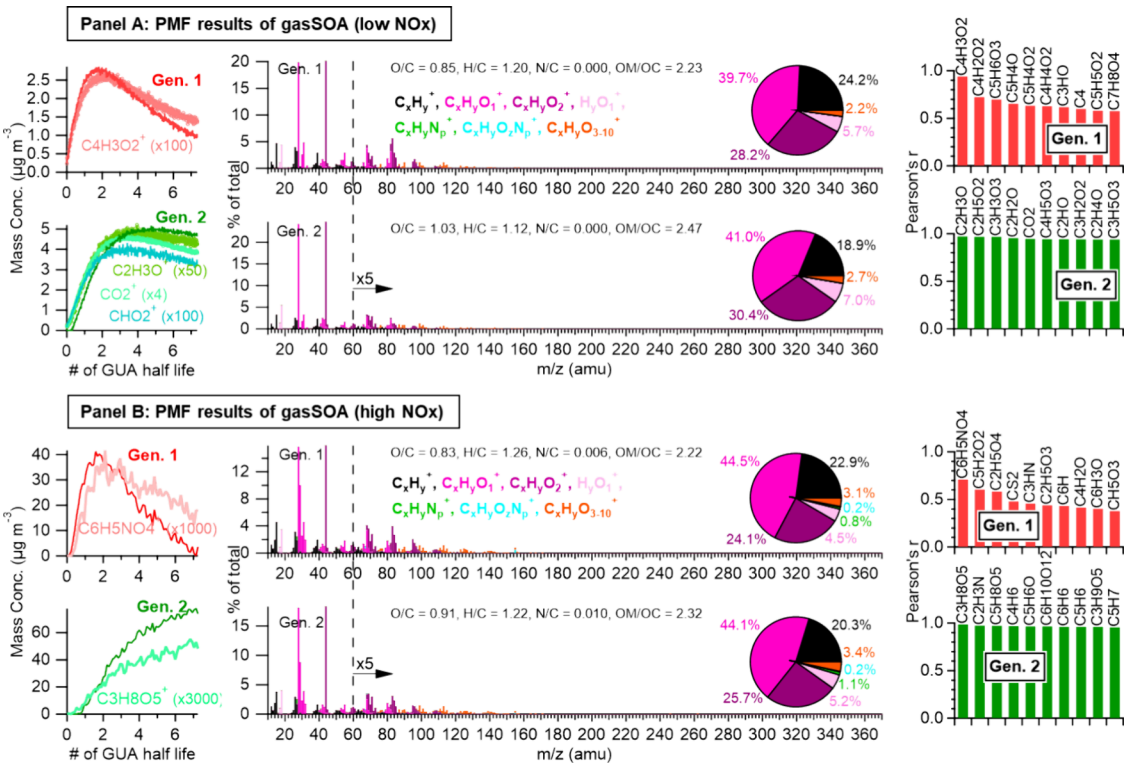

Figure 6. PMF results of gasSOA produced under low-NO_x (panel A) and high-NO_x (panel B) conditions, including time series and mass spectral profiles of different generations of gasSOA resolved by PMF and the correlation coefficients between the PMF factors and the AMS ions in gasSOA with the strongest correlations.

ization and fragmentation become more dominant during further aging.[40]

Previous studies have identified hydroxylation and carboxylic acid formation as important processes for phenol aqSOA formation.[38−40,54,55] Tracer ions representing guaiacol hydroxylation products (i.e., $C_7H_8O_3^+$ and $C_7H_8O_4^+$)[38] are observed in both guaiacol gasSOA and aqSOA (Figure 4g,h), suggesting that hydroxylation plays an important role in both gas-phase and aqueous-phase reactions of phenols.

Figure 4j,k shows the temporal trends of AMS tracers representing carboxylic acid and oxalic acid (i.e., CHO_2^+ and $CH_2O_2^+$, respectively).[54,56] In previous studies, the AMS signal at m/z 44 (mainly CO_2^+) has been widely used as a tracer for organic acids.[57−60] However, our current study indicates that the m/z 45 (CHO_2^+) signal might be a more reliable indicator of organic acids. To demonstrate this, Figure S6 shows the mass spectra from the National Institute of Standards and Technology (NIST) database for eight common small organic acids potentially present in atmospheric aerosols. These spectra consistently show a more prominent m/z 45 signal compared to the m/z 44 signal. While the thermal decomposition of carboxylic acids on the AMS vaporizer can result in a more pronounced CO_2^+ signal than that in NIST mass spectra,[57,61] carboxylic acids also yield a significant CHO_2^+ signal in AMS spectra, which allows us to use it as an acid indicator. Figures 5 and S7 show the time series of f_{CO2+} and f_{CHO2+} (the ratio of CO_2^+ and CHO_2^+ signals to the total organic signal in an AMS spectrum) alongside the total concentration of eight small organic acids measured by ion chromatography in guaiacol aqSOA. The stronger correlation between f_{CHO2+} and the total concentration of small acids indicates that f_{CHO2+} is an effective AMS marker for organic acids. CHO_2^+ is a better proxy of organic acids than CO_2^+ because the CO_2^+ signal can be influenced by other oxidized species (e.g., esters and peroxides)[62] and by artifacts from inorganic salts interacting with residual carbon on the vaporizer.[63] Therefore, CO_2^+ (or m/z 44) is less representative of organic acids than CHO_2^+, especially in highly oxidized SOA systems. Furthermore, $CH_2O_2^+$ (m/z 46) has been identified as an important AMS fragment of oxalic acid and oxalate and can serve as a reliable AMS tracer for aqueous-phase processing.[56]

As shown in Figure 4j,k, both CHO_2^+ and $CH_2O_2^+$ are initially elevated in guaiacol gasSOA but slightly decrease as the gas-phase reactions progress. In contrast, these acid tracers are nearly absent at the beginning of the aqueous-phase reactions but continuously increase throughout the reactions. These results indicate that the chemical compositions of aqSOA and gasSOA evolve differently during the process of photochemical reactions.

To systematically explore the chemical disparities between phenolic gasSOA and aqSOA and their photochemical evolution, we performed PMF analysis on the AMS spectra of guaiacol gasSOA and aqSOA from each experiment. For gasSOA generated under the low-NO_x and high-NO_x conditions (i.e., LN-gasSOA and HN-gasSOA), two factors were resolved, representing two generations of gasSOA products. For aqSOA generated through ^{3}C*- and •OH-mediated reactions (i.e., ^{3}C*-aqSOA and •OH-aqSOA), three distinct aqSOA factors were resolved.

Figure 6A shows the mass spectral profiles and temporal trends of the LN-gasSOA factors. The first-generation LN-gasSOA, characterized by lower oxidation levels (O/C = 0.85 and H/C = 1.20), peaks around 1.7 guaiacol half-lives, followed by a swift decline during the later period. The

https://doi.org/10.1021/acsearthspacechem.4c00204
ACS Earth Space Chem. 2024, 8, 2270−2283

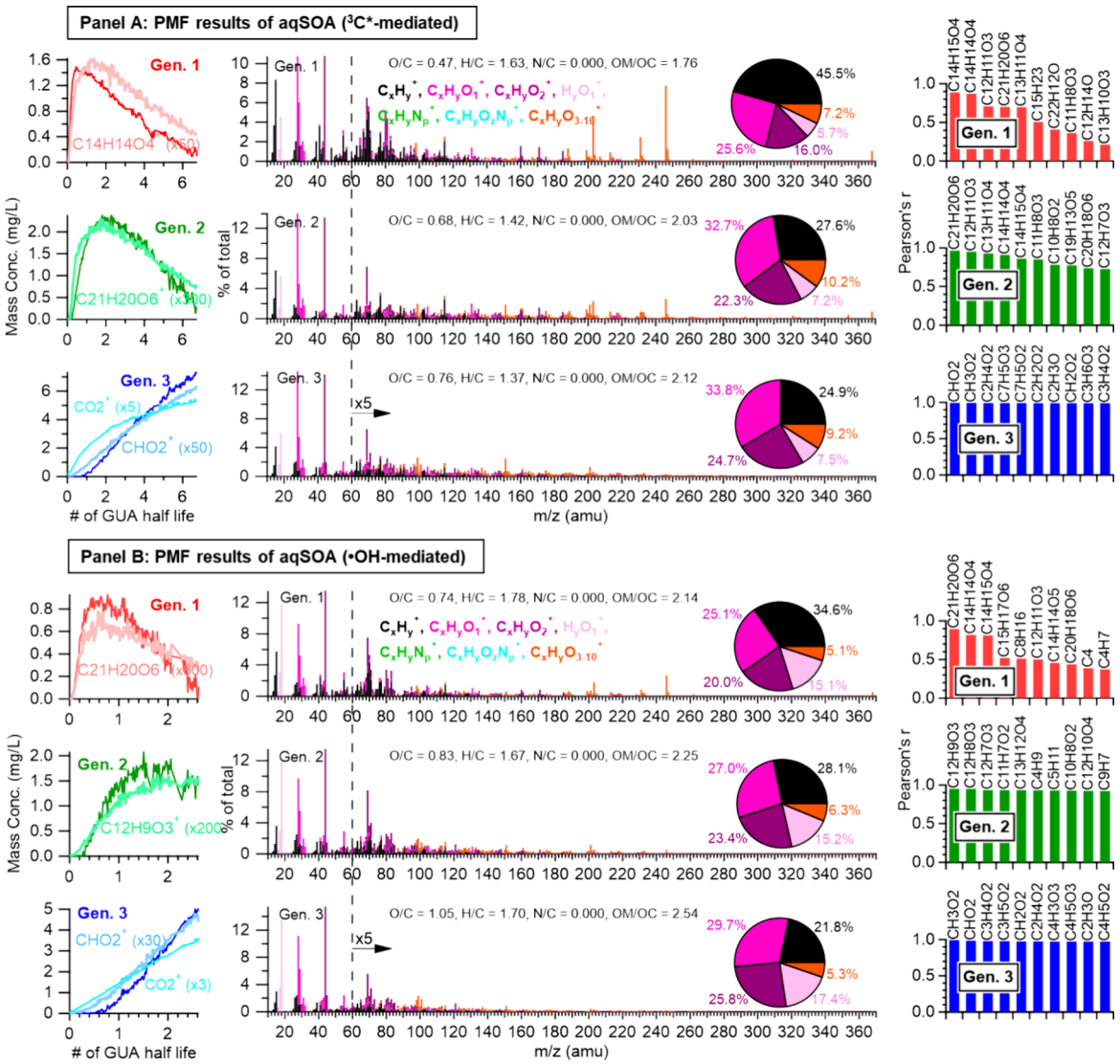

Figure 7. PMF results of the aqSOA produced from ^{3}C*-mediated (panel A) and •OH-mediated (panel B) photoreactions, including time series and mass spectral profiles of different generations of the aqSOA resolved by PMF and the correlation coefficients between the PMF factors and the AMS ions in aqSOA with the strongest correlations.

formation of the first-generation LN-gasSOA correlates well with a group of oxygenated C4 and C5 ions, such as $C_4H_3O_2^+$ (m/z 83), $C_4H_2O_2^+$ (m/z 82), and $C_5H_6O_3^+$ (m/z 114). In contrast, the second-generation LN-gasSOA, which is more oxidized (O/C = 1.03 and H/C = 1.12), peaks around four half-lives and shows a marginal decrease in concentration during a prolonged photoreaction. This second-generation LN-gasSOA is closely associated with smaller and more oxidized ions, such as $C_2H_3O^+$ (m/z 43), CO_2^+ (m/z 44), and $C_3H_3O_3^+$ (m/z 87). These findings suggest that under low-NO_x conditions, prolonged gas-phase photoreaction favors the formation of more oxidized and fragmented SOA products.

Figure 6B shows the mass spectra and time series of the HN-gasSOA factors. The first-generation HN-gasSOA peaks around 1.6 half-lives and exhibits lower oxidation levels (O/C = 0.86 and H/C = 1.24) compared to the second-generation HN-gasSOA (O/C = 0.93 and H/C = 1.22), which gradually increases in concentration over 6.5 half-lives. The mass spectra of the first-generation LN-gasSOA and HN-gasSOA are very similar for nearly all ion categories (i.e., $C_xH_y^+$, $C_xH_yO^+$, $C_xH_yO_2^+$, and $C_xH_yO_{>2}^+$; Figure S8). This strongly suggests that bulk chemical compositions of the initially formed LN-gasSOA and HN-gasSOA are very similar.

However, a key difference is observed in the mass spectrum of first-generation HN-gasSOA, which is closely associated with $C_6H_5NO_4^+$, likely a major fragment of nitrocatechol and its isomers. Furthermore, the first-generation HN-gasSOA shows an N/C ratio of 0.007, with $C_xH_yN_p^+$ and $C_xH_yO_zN_p^+$ ions constituting 0.8 and 0.2% of the mass spectrum, respectively. These observations indicate the production of nitroaromatics in the early stages of the gas-phase reaction under high-NO_x conditions. This finding is consistent with previous chamber studies that observed nitroaromatics formation from photooxidation of phenols in the presence of NO_x (Scheme S2).[37,64] However, $C_6H_5NO_4^+$ is significantly reduced in the second-generation HN-gasSOA, suggesting further chemical transformations of the nitroaromatics during a prolonged gas-phase reaction. Previous studies have found that both photolysis and •OH photooxidation can cause a rapid loss of nitrophenols and lead to photobleaching.[65,66]

Despite the decline in $C_6H_5NO_4^+$, the second-generation HN-gasSOA still exhibits a higher N/C ratio (0.010) than the

https://doi.org/10.1021/acsearthspacechem.4c00204
ACS Earth Space Chem. 2024, 8, 2270−2283

first-generation HN-gasSOA due to the increased mass fraction of $C_xH_yN_p^+$ ions (1.3%). This implies that further aging of the nitroaromatics in this study may produce other low-volatility N-containing organic compounds that persist in the aerosol phase.

Figure 7A illustrates the mass spectra and temporal profiles of the ^{3}C*-aqSOA factors. The first-generation ^{3}C*-aqSOA factor grows rapidly upon irradiation, reaching its peak around the one half-life of guaiacol and subsequently decreasing rapidly during the prolonged reaction. It is characterized as the least oxidized factor (O/C = 0.47 and H/C = 1.63), with its mass spectrum prominently featuring high m/z ions, including the AMS tracers of guaiacol oligomers (e.g., $C_{14}H_{14}O_4^+$ and $C_{21}H_{20}O_6^+$). This finding emphasizes the significance of oligomerization reactions in the early stages of the ^{3}C*-initiated aqueous-phase reaction. Oligomer ions also exist in the subsequent, more oxidized second-generation ^{3}C*-aqSOA factor, but their intensities notably diminish, indicating the decomposition of oligomers caused by prolonged photoreactions.

The third-generation ^{3}C*-aqSOA is the most oxidized (O/C = 0.76 and H/C = 1.37), with its mass spectrum showing negligible guaiacol oligomer ions. Instead, it correlates tightly with a group of small, oxygenated ions, such as CHO_2^+, $C_3HO_2^+$, and $CH_2O_2^+$, suggesting that carboxylic acid formation is increasingly important during extended aqueous-phase reactions. Specifically, the enhancement of $CH_2O_2^+$ is consistent with previous studies that identified $CH_2O_2^+$ as an important AMS fragment of oxalic acid and oxalate and proposed it as a reliable AMS tracer for aqueous-phase processing.[56] Similarly, •OH-aqSOA shows enhanced guaiacol oligomer ions in the mass spectra of the early-generation factors, whereas acid tracers and other small, oxygenated ions are more prevalent in the third-generation factor (Figure 7, panel B). Together, these findings suggest that fragmentation reactions are prominent processes during the later periods of aqueous-phase reactions, producing more oxidized products.

The mass spectra of guaiacol SOA factors reveal a high degree of similarity between the LN-gasSOA and HN-gasSOA factors. As shown in Figure S8a, the correlation coefficient is 0.92 between the first-generation LN-gasSOA and HN-gasSOA and 0.94 between the second generations. This result suggests the shared gasSOA products and gas-phase reaction pathways under low- and high-NOx conditions. Additionally, the similarity between different generation gasSOA factors implies a relatively minor chemical alteration during prolonged gas-phase reactions. However, there is little similarity between aqSOA and gasSOA factors, especially among the early-generation factors. For example, the correlation coefficient between the first-generation LN-gasSOA and the first-generation ^{3}C*-aqSOA is only 0.08 for ions larger than 60 amu (Figure S8). The low MS similarity, particularly in the high m/z range, underscores prominent oligomerization during the initial stage of aqueous-phase reactions, which is not observed in gas-phase reactions. Additionally, among all ion categories, the $C_xH_y^+$ and $C_xH_yO_{>2}^+$ ions demonstrate the most notable differences between different generations of aqSOA and gasSOA (Figure S8).

3.4. Differences in Formation Mechanisms between Guaiacol AqSOA and GasSOA. *3.4.1. Formation of Oligomers in AqSOA.* The variation in oligomer formation between guaiacol gasSOA and aqSOA is further substantiated through ESI-TOF-MS and nano-DESI-MS analyses,[29,38] which provide detailed molecular insights into the components of gasSOA and aqSOA. As demonstrated in Tables S1 and S2, the ten most abundant products identified in guaiacol aqSOA comprise guaiacol dimers, trimers, and their derivatives. Among these, the molecules with the formulas of $C_{14}H_{14}O_4$ and $C_{14}H_{14}O_6$, representing guaiacol dimer and hydroxylated dimer, respectively, are the two most abundant products in guaiacol aqSOA generated in the early stages of photoreactions.

In contrast, no oligomers were observed in the ESI-TOF-MS analysis of guaiacol gasSOA. As shown in Tables S3 and S4, under low-NO_x conditions, the major gasSOA products consist of functionalized guaiacol monomers and ring-opening products, whereas under high-NO_x conditions, N-containing products, likely from the nitration of guaiacols, are more prominent.

The enhanced oligomerization observed in aqueous-phase reactions can be attributed to a higher fraction of phenoxy radicals undergoing radical coupling. As shown in Scheme S1, in both the gas and aqueous phases, phenoxy radicals are formed upon hydrogen abstraction, and the subsequent coupling of these radicals leads to oligomer formation. However, in the gas phase, phenoxy radicals can also react rapidly with ozone, NO, and NO_2. These competing reactions may result in a shorter lifetime of phenoxy radicals in the gas phase, leading to limited oligomerization. It is important to note that the gasSOA photoreaction experiments in this study were conducted under dry conditions (RH < 10%), which is significantly lower than the typical ambient conditions. Further research is needed to investigate potential oligomerization in phenolic gasSOA under higher humidities.

3.4.2. Formation of Carboxylic Acids in AqSOA and GasSOA. Carboxylic acids constitute a significant fraction of SOA, particularly in aged SOA.[48,67] Both gas-phase and aqueous-phase reactions generate organic acids during SOA formation.[38,68,69] Figure 4j shows the time series of f_{CHO2+} (the indicator of organic acids) for both gasSOA and aqSOA during the reactions. Initially, the organic acid content is higher in guaiacol gasSOA than in aqSOA. As the reactions progress, the acid fraction in gasSOA remains stable, whereas it significantly increases in aqSOA. Notably, the organic acid fraction in •OH-aqSOA surpasses that in gasSOA after one half-life of guaiacol and continues to grow with a continued reaction time. Meanwhile, the rise of f_{CHO2+} in ^{3}C*-mediated aqSOA is more gradual but increases throughout the entire experiment. These observations suggest that aqueous-phase photooxidation could serve as an important and continuous source of carboxylic acids in BB smoke.

Likewise, previous research has revealed the pivotal role of liquid water in facilitating the formation of acids from aromatic precursors. For example, Dong et al. demonstrated that the gas-phase photooxidation of toluene preferentially produces glyoxal and methylglyoxal, whereas aqueous-phase reactions are more likely to produce formic and acetic acids.[70] Similarly, Faust et al. observed the increased yields of glyoxal and glyoxylic acid from toluene photooxidation in the presence of deliquesced seed particles as opposed to dry seeds.[71]

The enhanced formation of acids in the aqueous phase can be attributed to the formation of distinct intermediates formed during gas- and aqueous-phase reactions, with hydration occurring exclusively in the latter. As demonstrated in Schemes S1 and S3, a crucial intermediate in the gas phase is a bicyclic radical with a five-membered oxygen bridge ring (BR-5), which

https://doi.org/10.1021/acsearthspacechem.4c00204
ACS Earth Space Chem. 2024, 8, 2270−2283

mainly leads to aldehyde formation during the subsequent ring-opening reactions.[72] However, the presence of liquid water facilitates the formation of a bicyclic radical with a six-membered oxygen bridge ring (BR-6).[70] The formation of a peroxy radical−water complex transition state lowers the energy barrier for BR-6 formation.[73] Ring-opening reactions of BR-6 produce acyl radicals, which readily undergo hydration in the aqueous phase,[74] resulting in α-hydroxy peroxy radicals upon the addition of O_2. The subsequent elimination of HO_2 from α-hydroxy peroxy radicals ultimately results in the formation of carboxylic acids. This distinction in reaction intermediates and pathways also agrees with our observation of a higher f_{C2H3O+} in gasSOA compared to aqSOA (Figure 4l). The $C_2H_3O^+$ ion (either CH_2CHO^+ or $COCH_3^+$) is known to be produced from the fragmentation of aldehydes and ketones and has been commonly used as a marker for nonacid oxygenates.[61,75] The elevated f_{C2H3O+} in gasSOA indicates that aldehyde formation is more prevalent in gas-phase reactions, whereas acid formation is favored in aqueous-phase reactions. These findings underscore the critical role of liquid water in driving the acid formation processes.

3.5. AMS Tracer Ions for Phenolic AqSOA and GasSOA. Signature ions and tracers in aerosol mass spectra are widely utilized to identify and quantify contributions from various aerosol sources and chemical processes.[76−80] Since AMS uses 70 eV EI, which ionizes and fragments molecules in a reproducible pattern, specific AMS ion fragments are characteristic of certain compounds or compound classes and can serve as reliable source indicators. For example, $C_5H_6O^+$ (m/z 82) is notably enhanced in the mass spectra of IEPOX-SOA and is recognized as a key tracer for IEPOX-SOA.[77] By applying multivariate statistical techniques, such as PMF, to ambient AMS data, complex aerosol mass spectra can be decomposed into individual factors corresponding to different sources and formation pathways.[46,47] These signature ions and tracers can help validate the resolved factors, enhancing the accuracy and reliability of the source apportionment models.

As discussed in earlier sections, the AMS spectra of guaiacol gasSOA and aqSOA differ significantly due to their distinct formation mechanisms that lead to variations in the chemical composition. In light of this, we propose a set of AMS ions that could serve as effective tracers for gasSOA and aqSOA originating from BB-related phenols in the atmosphere. However, it is important to further evaluate the validity of these proposed AMS tracers by examining the ambient organic aerosol mass spectrometry data.

The AMS spectra of early-stage guaiacol aqSOA exhibit distinct and prominent high m/z ions, including $C_{11}H_7O_2^+$, $C_{12}H_{11}O_3^+$, $C_{13}H_{11}O_4^+$, $C_{14}H_{14}O_4^+$, $C_{14}H_{14}O_5^+$, and $C_{21}H_{20}O_6^+$. These ions arise from the fragmentation of oligomeric products formed during the initial aqueous-phase photoreactions,[38] making them effective tracers for phenolic aqSOA. Additionally, we have identified several other ions—$C_9H_7O^+$, $C_8H_7O_3^+$, $C_{12}H_9O_2^+$, $C_{11}H_9O_3^+$, $C_{12}H_9O_3^+$, and $C_{13}H_9O_3^+$—that are enhanced in the spectra of guaiacol aqSOA but absent in guaiacol gasSOA (Figure S9). Unlike the oligomer ions, which decline quickly and are depleted during the later stage of photoreactions, these ions remain elevated throughout the entire reaction period. Notably, the $C_8H_7O_3^+$ ion shows an increase in its activity over time. Considering their consistent presence in the mass spectra of guaiacol aqSOA and their near absence in gasSOA, these ions could serve as AMS tracer ions for phenolic aqSOA.

Conversely, the AMS spectra of guaiacol gasSOA feature a distinct cluster of $C_xH_yO_1^+$ ions (e.g., $C_4H_4O^+$ and $C_5H_4O^+$) and $C_xH_yO_2^+$ ions (e.g., $C_2H_3O_2^+$, $C_3H_2O_2^+$, $C_3H_3O_2^+$, $C_4H_3O_2^+$, $C_4H_4O_2^+$, $C_4H_5O_2^+$, and $C_5H_3O_2^+$) in the m/z range of 59−96, which are likely produced from aldehydes and ketones that contain one or multiple nonacid carbonyl groups. These ions are significantly less abundant in the mass spectra of guaiacol aqSOA compared to gasSOA throughout the entire duration of the photoreaction, from the onset of the reaction until nearly all of the guaiacol precursor has reacted (Figure 4). Therefore, these ions may serve as effective AMS tracers for phenolic gasSOA.

4. CONCLUSIONS

This study investigates the chemical differences between gasSOA and aqSOA formed from the photochemical reactions of guaiacol. Initially, gasSOA exhibits higher levels of oxidation and elevated acid formation compared to aqSOA. However, as gas-phase reactions progress, the oxidation degree and the abundance of carboxylates in gasSOA remain relatively stable, whereas extended aqueous-phase reactions lead to notable increases in the oxidation degree and acid formation within aqSOA.

Oligomers are present in guaiacol aqSOA but conspicuously absent in gasSOA, indicating that oligomerization is significant in aqueous-phase reactions but may not be prevalent in gas-phase reactions. Therefore, the presence of oligomeric ions and a set of other high m/z ions in AMS spectra, such as $C_{14}H_{14}O_4^+$, $C_{12}H_9O_3^+$, $C_9H_7O^+$, $C_8H_7O_3^+$, etc., may serve as AMS tracers for distinguishing between phenolic gasSOA and aqSOA. However, since gasSOA was generated under dry conditions (RH < 10%) in this study, further research is necessary to investigate potential oligomerization in phenolic gasSOA under higher RH conditions.

Within liquid water, processes such as hydration and hydrolysis play important roles in the generation of aqSOA.[20,81] Accretion reactions, such as aldol condensation, esterification, acetal and hemiacetal formation, and various extents of oligomerizations, can be notably intensified in aqueous-phase reactions.[19] Furthermore, the formation of hydrogen bonds between water and reactants, which may include precursors, reaction intermediates, and transition states, can influence reaction barriers and thereby modulate reaction rates and branching.[82] The present study highlights that the chemical compositions and reaction kinetics of gasSOA and aqSOA can diverge significantly, even when derived from the same precursor. Understanding these differences is crucial for accurately simulating SOA in atmospheric models and assessing their implications on air quality and public health.

■ ASSOCIATED CONTENT

Supporting Information

The Supporting Information is available free of charge at https://pubs.acs.org/doi/10.1021/acsearthspacechem.4c00204.

Additional details on PMF analysis, experimental conditions of the photochemical reactions, molecular information on major guaiacol gasSOA and aqSOA products, correlations between the mass spectra of different generations of guaiacol gasSOA and aqSOA, EI mass spectra of small organic acids, correlation between

https://doi.org/10.1021/acsearthspacechem.4c00204
ACS Earth Space Chem. 2024, 8, 2270−2283

the AMS-measured f_{CHO2+} and the total concentration of small acids in guaiacol aqSOA, and formation mechanisms of bicyclic radicals in gas and aqueous-phase reactions of phenols (PDF)

AUTHOR INFORMATION

Corresponding Author

Qi Zhang − *Department of Environmental Toxicology, University of California, Davis, California 95616, United States; Agricultural and Environmental Chemistry Graduate Group, University of California, Davis, California 95616, United States;* orcid.org/0000-0002-5203-8778; Email: dkwzhang@ucdavis.edu

Authors

Wenqing Jiang − *Department of Environmental Toxicology, University of California, Davis, California 95616, United States; Agricultural and Environmental Chemistry Graduate Group, University of California, Davis, California 95616, United States;* orcid.org/0000-0002-6869-3232

Lu Yu − *Department of Environmental Toxicology, University of California, Davis, California 95616, United States; Agricultural and Environmental Chemistry Graduate Group, University of California, Davis, California 95616, United States*

Lindsay Yee − *Division of Engineering and Applied Science, California Institute of Technology, Pasadena, California 91125, United States;* Present Address: Currently at Department of Environmental Science, Policy, and Management, University of California, Berkeley, CA, United States; orcid.org/0000-0001-8965-9319

Puneet Chhabra − *Department of Chemistry and Chemical Engineering, California Institute of Technology, Pasadena, California 91125, United States;* Present Address: Currently at Yale School of Management, New Haven, CT, United States.

John Seinfeld − *Division of Engineering and Applied Science and Department of Chemistry and Chemical Engineering, California Institute of Technology, Pasadena, California 91125, United States;* orcid.org/0000-0003-1344-4068

Cort Anastasio − *Agricultural and Environmental Chemistry Graduate Group, University of California, Davis, California 95616, United States; Department of Land, Air, and Water Resources, University of California, Davis, California 95616-8627, United States;* orcid.org/0000-0002-5373-0459

Complete contact information is available at: https://pubs.acs.org/10.1021/acsearthspacechem.4c00204

Notes

The authors declare no competing financial interest.

ACKNOWLEDGMENTS

This work was supported by grants from the US Department of Energy Atmospheric System Research Program (DE-SC0022140), the National Science Foundation (grant No. AGS-2220307), and the California Agricultural Experiment Station (CA-D-ETX-2102-H and CA-D-LAW-6403-RR). W.J. also acknowledges funding from the Jastro-Shields Research Award, the Donald G. Crosby Fellowship in Environmental Chemistry, and the Fumio Matsumura Memorial Fellowship from the University of California at Davis. The authors gratefully acknowledge Matthew Coggon (NOAA) for sharing their data.

REFERENCES

(1) Zhang, Q.; Jimenez, J. L.; Canagaratna, M. R.; Allan, J. D.; Coe, H.; Ulbrich, I.; Alfarra, M. R.; Takami, A.; Middlebrook, A. M.; Sun, Y. L.; Dzepina, K.; Dunlea, E.; Docherty, K.; DeCarlo, P. F.; Salcedo, D.; Onasch, T.; Jayne, J. T.; Miyoshi, T.; Shimono, A.; Hatakeyama, S.; Takegawa, N.; Kondo, Y.; Schneider, J.; Drewnick, F.; Borrmann, S.; Weimer, S.; Demerjian, K.; Williams, P.; Bower, K.; Bahreini, R.; Cottrell, L.; Griffin, R. J.; Rautiainen, J.; Sun, J. Y.; Zhang, Y. M.; Worsnop, D. R. Ubiquity and Dominance of Oxygenated Species in Organic Aerosols in Anthropogenically-Influenced Northern Hemisphere Midlatitudes. *Geophys. Res. Lett.* **2007**, *34* (13), L13801.

(2) Jimenez, J. L.; Canagaratna, M. R.; Donahue, N. M.; Prevot, A. S. H.; Zhang, Q.; Kroll, J. H.; DeCarlo, P. F.; Allan, J. D.; Coe, H.; Ng, N. L.; Aiken, A. C.; Docherty, K. S.; Ulbrich, I. M.; Grieshop, A. P.; Robinson, A. L.; Duplissy, J.; Smith, J. D.; Wilson, K. R.; Lanz, V. A.; Hueglin, C.; Sun, Y. L.; Tian, J.; Laaksonen, A.; Raatikainen, T.; Rautiainen, J.; Vaattovaara, P.; Ehn, M.; Kulmala, M.; Tomlinson, J. M.; Collins, D. R.; Cubison, M. J.; Dunlea, J.; Huffman, J. A.; Onasch, T. B.; Alfarra, M. R.; Williams, P. I.; Bower, K.; Kondo, Y.; Schneider, J.; Drewnick, F.; Borrmann, S.; Weimer, S.; Demerjian, K.; Salcedo, D.; Cottrell, L.; Griffin, R.; Takami, A.; Miyoshi, T.; Hatakeyama, S.; Shimono, A.; Sun, J. Y.; Zhang, Y. M.; Dzepina, K.; Kimmel, J. R.; Sueper, D.; Jayne, J. T.; Herndon, S. C.; Trimborn, A. M.; Williams, L. R.; Wood, E. C.; Middlebrook, A. M.; Kolb, C. E.; Baltensperger, U.; Worsnop, D. R. Evolution of Organic Aerosols in the Atmosphere. *Science* **2009**, *326* (5959), 1525−1529.

(3) Hallquist, M.; Wenger, J. C.; Baltensperger, U.; Rudich, Y.; Simpson, D.; Claeys, M.; Dommen, J.; Donahue, N. M.; George, C.; Goldstein, A. H.; Hamilton, J. F.; Herrmann, H.; Hoffmann, T.; Iinuma, Y.; Jang, M.; Jenkin, M. E.; Jimenez, J. L.; Kiendler-Scharr, A.; Maenhaut, W.; McFiggans, G.; Mentel, T. F.; Monod, A.; Prévôt, A. S. H.; Seinfeld, J. H.; Surratt, J. D.; Szmigielski, R.; Wildt, J. The Formation, Properties and Impact of Secondary Organic Aerosol: Current and Emerging Issues. *Atmos. Chem. Phys.* **2009**, *9* (14), 5155−5236.

(4) Shrivastava, M.; Cappa, C. D.; Fan, J.; Goldstein, A. H.; Guenther, A. B.; Jimenez, J. L.; Kuang, C.; Laskin, A.; Martin, S. T.; Ng, N. L.; Petaja, T.; Pierce, J. R.; Rasch, P. J.; Roldin, P.; Seinfeld, J. H.; Shilling, J.; Smith, J. N.; Thornton, J. A.; Volkamer, R.; Wang, J.; Worsnop, D. R.; Zaveri, R. A.; Zelenyuk, A.; Zhang, Q. Recent Advances in Understanding Secondary Organic Aerosol: Implications for Global Climate Forcing. *Rev. Geophys.* **2017**, *55* (2), 509−559.

(5) Xu, B.; Zhang, G.; Gustafsson, Ö.; Kawamura, K.; Li, J.; Andersson, A.; Bikkina, S.; Kunwar, B.; Pokhrel, A.; Zhong, G.; Zhao, S.; Li, J.; Huang, C.; Cheng, Z.; Zhu, S.; Peng, P.; Sheng, G. Large Contribution of Fossil-Derived Components to Aqueous Secondary Organic Aerosols in China. *Nat. Commun.* **2022**, *13* (1), 1−12.

(6) El-Sayed, M. M. H.; Hennigan, C. J. Aqueous Processing of Water-Soluble Organic Compounds in the Eastern United States during Winter. *Environ. Sci. Process. Impacts* **2023**, *25* (2), 241−253.

(7) Wang, J.; Ye, J.; Zhang, Q.; Zhao, J.; Wu, Y.; Li, J.; Liu, D.; Li, W.; Zhang, Y.; Wu, C.; Xie, C.; Qin, Y.; Lei, Y.; Huang, X.; Guo, J.; Liu, P.; Fu, P.; Li, Y.; Lee, H. C.; Choi, H.; Zhang, J.; Liao, H.; Chen, M.; Sun, Y.; Ge, X.; Martin, S. T.; Jacob, D. J. Aqueous Production of Secondary Organic Aerosol from Fossil-Fuel Emissions in Winter Beijing Haze. *Proc. Natl. Acad. Sci. U. S. A.* **2021**, *118* (8), 1−6.

(8) Wonaschuetz, A.; Sorooshian, A.; Ervens, B.; Chuang, P. Y.; Feingold, G.; Murphy, S. M.; De Gouw, J.; Warneke, C.; Jonsson, H. H. Aerosol and Gas Re-Distribution by Shallow Cumulus Clouds: An Investigation Using Airborne Measurements. *J. Geophys. Res. Atmos.* **2012**, *117* (17), 1−18.

(9) Coeur-Tourneur, C.; Cassez, A.; Wenger, J. C. Rate Coefficients for the Gas-Phase Reaction of Hydroxyl Radicals with 2-Methoxyphenol (Guaiacol) and Related Compounds. *J. Phys. Chem. A* **2010**, *114* (43), 11645−11650.

(10) Smith, J. D.; Kinney, H.; Anastasio, C. Aqueous Benzene-Diols React with an Organic Triplet Excited State and Hydroxyl Radical to Form Secondary Organic Aerosol. *Phys. Chem. Chem. Phys.* **2015**, *17* (15), 10227−10237.
(11) Kaur, R.; Anastasio, C. First Measurements of Organic Triplet Excited States in Atmospheric Waters. *Environ. Sci. Technol.* **2018**, *52* (9), 5218−5226.
(12) Ma, L.; Guzman, C.; Niedek, C.; Tran, T.; Zhang, Q.; Anastasio, C. Kinetics and Mass Yields of Aqueous Secondary Organic Aerosol from Highly Substituted Phenols Reacting with a Triplet Excited State. *Environ. Sci. Technol.* **2021**, *55* (9), 5772−5781.
(13) Zhang, J.; Shrivastava, M.; Ma, L.; Jiang, W.; Anastasio, C.; Zhang, Q.; Zelenyuk, A. Modeling Novel Aqueous Particle and Cloud Chemistry Processes of Biomass Burning Phenols and Their Potential to Form Secondary Organic Aerosols. *Environ. Sci. Technol.* **2024**, *58* (8), 3776−3786.
(14) McNeill, V. F. Aqueous Organic Chemistry in the Atmosphere: Sources and Chemical Processing of Organic Aerosols. *Environ. Sci. Technol.* **2015**, *49* (3), 1237−1244.
(15) Smith, J. D.; Sio, V.; Yu, L.; Zhang, Q.; Anastasio, C. Secondary Organic Aerosol Production from Aqueous Reactions of Atmospheric Phenols with an Organic Triplet Excited State. *Environ. Sci. Technol.* **2014**, *48* (2), 1049−1057.
(16) Ortiz-Montalvo, D. L.; Lim, Y. B.; Perri, M. J.; Seitzinger, S. P.; Turpin, B. J. Volatility and Yield of Glycolaldehyde SOA Formed through Aqueous Photochemistry and Droplet Evaporation. *Aerosol Sci. Technol.* **2012**, *46* (9), 1002−1014.
(17) Ervens, B.; Turpin, B. J.; Weber, R. J. Secondary Organic Aerosol Formation in Cloud Droplets and Aqueous Particles (AqSOA): A Review of Laboratory, Field and Model Studies. *Atmos. Chem. Phys.* **2011**, *11* (21), 11069−11102.
(18) Ervens, B. Modeling the Processing of Aerosol and Trace Gases in Clouds and Fogs. *Chem. Rev.* **2015**, *115* (10), 4157−4198.
(19) Herrmann, H.; Schaefer, T.; Tilgner, A.; Styler, S. A.; Weller, C.; Teich, M.; Otto, T. Tropospheric Aqueous-Phase Chemistry: Kinetics, Mechanisms, and Its Coupling to a Changing Gas Phase. *Chem. Rev.* **2015**, *115* (10), 4259−4334.
(20) Lim, Y. B.; Tan, Y.; Perri, M. J.; Seitzinger, S. P.; Turpin, B. J. Aqueous Chemistry and Its Role in Secondary Organic Aerosol (SOA) Formation. *Atmos. Chem. Phys.* **2010**, *10* (21), 10521−10539.
(21) Bateman, A. P.; Nizkorodov, S. A.; Laskin, J.; Laskin, A. Photolytic Processing of Secondary Organic Aerosols Dissolved in Cloud Droplets. *Phys. Chem. Chem. Phys.* **2011**, *13* (26), 12199−12212.
(22) Michaud, V.; Haddad, I. E.; Liu, Y.; Sellegri, K.; Laj, P.; Villani, P.; Picard, D.; Marchand, N.; Monod, A. In-Cloud Processes of Methacrolein under Simulated Conditions—Part 3: Hygroscopic and Volatility Properties of the Formed Secondary Organic Aerosol. *Atmos. Chem. Phys.* **2009**, *9* (14), 5119−5130.
(23) Pöschl, U.; Shiraiwa, M. Multiphase Chemistry at the Atmosphere-Biosphere Interface Influencing Climate and Public Health in the Anthropocene. *Chem. Rev.* **2015**, *115* (10), 4440−4475.
(24) Fu, T.-M.; Jacob, D. J.; Heald, C. L. Aqueous-Phase Reactive Uptake of Dicarbonyls as a Source of Organic Aerosol over Eastern North America. *Atmos. Environ.* **2009**, *43* (10), 1814−1822.
(25) Fu, T.-M.; Jacob, D. J.; Wittrock, F.; Burrows, J. P.; Vrekoussis, M.; Henze, D. K. Global Budgets of Atmospheric Glyoxal and Methylglyoxal, and Implications for Formation of Secondary Organic Aerosols. *J. Geophys. Res. Atmos.* **2008**, *113* (D15). .
(26) Woo, J. L.; Kim, D. D.; Schwier, A. N.; Li, R.; McNeill, V. F. Aqueous Aerosol SOA Formation: Impact on Aerosol Physical Properties. *Faraday Discuss.* **2013**, *165* (0), 357−367.
(27) Wang, Y.; Jorga, S.; Abbatt, J. Nitration of Phenols by Reaction with Aqueous Nitrite: A Pathway for the Formation of Atmospheric Brown Carbon. *ACS Earth Sp. Chem.* **2023**, *7* (3), 632−641.
(28) Schauer, J. J.; Cass, G. R. Source Apportionment of Wintertime Gas-Phase and Particle-Phase Air Pollutants Using Organic Compounds as Tracers. *Environ. Sci. Technol.* **2000**, *34* (9), 1821−1832.
(29) Yee, L. D.; Kautzman, K. E.; Loza, C. L.; Schilling, K. A.; Coggon, M. M.; Chhabra, P. S.; Chan, M. N.; Chan, A. W. H.; Hersey, S. P.; Crounse, J. D.; Wennberg, P. O.; Flagan, R. C.; Seinfeld, J. H. Secondary Organic Aerosol Formation from Biomass Burning Intermediates: Phenol and Methoxyphenols. *Atmos. Chem. Phys.* **2013**, *13* (16), 8019−8043.
(30) Ofner, J.; Krüger, H. U.; Grothe, H.; Schmitt-Kopplin, P.; Whitmore, K.; Zetzsch, C. Physico-Chemical Characterization of SOA Derived from Catechol and Guaiacol - a Model Substance for the Aromatic Fraction of Atmospheric HULIS. *Atmos. Chem. Phys.* **2011**, *11* (1), 1−15.
(31) Nakao, S.; Clark, C.; Tang, P.; Sato, K.; Cocker, D., III Secondary Organic Aerosol Formation from Phenolic Compounds in the Absence of NO_X. *Atmos. Chem. Phys.* **2011**, *11* (20), 10649−10660.
(32) McFall, A. S.; Johnson, A. W.; Anastasio, C. Air−Water Partitioning of Biomass-Burning Phenols and the Effects of Temperature and Salinity. *Environ. Sci. Technol.* **2020**, *54* (7), 3823−3830.
(33) Arciva, S.; Niedek, C.; Mavis, C.; Yoon, M.; Sanchez, M. E.; Zhang, Q.; Anastasio, C. Aqueous ·OH Oxidation of Highly Substituted Phenols as a Source of Secondary Organic Aerosol. *Environ. Sci. Technol.* **2022**, *56* (14), 9959−9967.
(34) Kaur, R.; Labins, J. R.; Helbock, S. S.; Jiang, W.; Bein, K. J.; Zhang, Q.; Anastasio, C. Photooxidants from Brown Carbon and Other Chromophores in Illuminated Particle Extracts. *Atmos. Chem. Phys.* **2019**, *19* (9), 6579−6594.
(35) Xiao, Y.; Hu, M.; Li, X.; Zong, T.; Xu, N.; Hu, S.; Zeng, L.; Chen, S.; Song, Y.; Guo, S.; Wu, Z. Aqueous Secondary Organic Aerosol Formation Attributed to Phenols from Biomass Burning. *Sci. Total Environ.* **2022**, *847*, No. 157582.
(36) Simpson, C. D.; Naeher, L. P. Biological Monitoring of Wood-Smoke Exposure. *Inhal. Toxicol.* **2010**, *22* (2), 99−103.
(37) Lauraguais, A.; Coeur-Tourneur, C.; Cassez, A.; Deboudt, K.; Fourmentin, M.; Choël, M. Atmospheric Reactivity of Hydroxyl Radicals with Guaiacol (2-Methoxyphenol), a Biomass Burning Emitted Compound: Secondary Organic Aerosol Formation and Gas-Phase Oxidation Products. *Atmos. Environ.* **2014**, *86*, 155−163.
(38) Yu, L.; Smith, J.; Laskin, A.; Anastasio, C.; Laskin, J.; Zhang, Q. Chemical Characterization of SOA Formed from Aqueous-Phase Reactions of Phenols with the Triplet Excited State of Carbonyl and Hydroxyl Radical. *Atmos. Chem. Phys.* **2014**, *14* (24), 13801−13816.
(39) Sun, Y. L.; Zhang, Q.; Anastasio, C.; Sun, J. Insights into Secondary Organic Aerosol Formed via Aqueous-Phase Reactions of Phenolic Compounds Based on High Resolution Mass Spectrometry. *Atmos. Chem. Phys.* **2010**, *10* (10), 4809−4822.
(40) Yu, L.; Smith, J.; Laskin, A.; George, K. M.; Anastasio, C.; Laskin, J.; Dillner, A. M.; Zhang, Q. Molecular Transformations of Phenolic SOA during Photochemical Aging in the Aqueous Phase: Competition among Oligomerization, Functionalization, and Fragmentation. *Atmos. Chem. Phys.* **2016**, *16* (7), 4511−4527.
(41) George, K. M.; Ruthenburg, T. C.; Smith, J.; Yu, L.; Zhang, Q.; Anastasio, C.; Dillner, A. M. FT-IR Quantification of the Carbonyl Functional Group in Aqueous-Phase Secondary Organic Aerosol from Phenols. *Atmos. Environ.* **2015**, *100*, 230−237.
(42) Sun, J.; Mu, Q.; Kimura, H.; Murugadoss, V.; He, M.; Du, W.; Hou, C. Oxidative Degradation of Phenols and Substituted Phenols in the Water and Atmosphere: A Review. *Adv. Compos. Hybrid Mater.* **2022**, *5* (2), 627−640.
(43) Anastasio, C.; Faust, B. C.; Rao, C. J. Aromatic Carbonyl Compounds as Aqueous-Phase Photochemical Sources of Hydrogen Peroxide in Acidic Sulfate Aerosols, Fogs, and Clouds. 1. Non-Phenolic Methoxybenzaldehydes and Methoxyacetophenones with Reductants (Phenols). *Environ. Sci. Technol.* **1997**, *31* (1), 218−232.
(44) Aiken, A. C.; DeCarlo, P. F.; Kroll, J. H.; Worsnop, D. R.; Huffman, J. A.; Docherty, K. S.; Ulbrich, I. M.; Mohr, C.; Kimmel, J. R.; Sueper, D.; Sun, Y.; Zhang, Q.; Trimborn, A.; Northway, M.; Ziemann, P. J.; Canagaratna, M. R.; Onasch, T. B.; Alfarra, M. R.; Prevot, A. S. H.; Dommen, J.; Duplissy, J.; Metzger, A.; Baltensperger, U.; Jimenez, J. L. O/C and OM/OC Ratios of Primary, Secondary,

https://doi.org/10.1021/acsearthspacechem.4c00204
ACS Earth Space Chem. 2024, 8, 2270−2283

and Ambient Organic Aerosols with High-Resolution Time-of-Flight Aerosol Mass Spectrometry. *Environ. Sci. Technol.* **2008**, *42* (12), 4478−4485.
(45) Kroll, J. H.; Donahue, N. M.; Jimenez, J. L.; Kessler, S. H.; Canagaratna, M. R.; Wilson, K. R.; Altieri, K. E.; Mazzoleni, L. R.; Wozniak, A. S.; Bluhm, H.; Mysak, E. R.; Smith, J. D.; Kolb, C. E.; Worsnop, D. R. Carbon Oxidation State as a Metric for Describing the Chemistry of Atmospheric Organic Aerosol. *Nat. Chem.* **2011**, *3* (2), 133−139.
(46) Ulbrich, I. M.; Canagaratna, M. R.; Zhang, Q.; Worsnop, D. R.; Jimenez, J. L. Interpretation of Organic Components from Positive Matrix Factorization of Aerosol Mass Spectrometric Data. *Atmos. Chem. Phys.* **2009**, *9* (9), 2891−2918.
(47) Zhang, Q.; Jimenez, J. L.; Canagaratna, M. R.; Ulbrich, I. M.; Ng, N. L.; Worsnop, D. R.; Sun, Y. Understanding Atmospheric Organic Aerosols via Factor Analysis of Aerosol Mass Spectrometry: A Review. *Anal. Bioanal. Chem.* **2011**, *401* (10), 3045−3067.
(48) Heald, C. L.; Kroll, J. H.; Jimenez, J. L.; Docherty, K. S.; DeCarlo, P. F.; Aiken, A. C.; Chen, Q.; Martin, S. T.; Farmer, D. K.; Artaxo, P. A Simplified Description of the Evolution of Organic Aerosol Composition in the Atmosphere. *Geophys. Res. Lett.* **2010**, *37* (8), L08803.
(49) Chan, A. W. H.; Kroll, J. H.; Ng, N. L.; Seinfeld, J. H. Kinetic Modeling of Secondary Organic Aerosol Formation: Effects of Particle- and Gas-Phase Reactions of Semivolatile Products. *Atmos. Chem. Phys.* **2007**, *7* (15), 4135−4147.
(50) Shilling, J. E.; Chen, Q.; King, S. M.; Rosenoern, T.; Kroll, J. H.; Worsnop, D. R.; DeCarlo, P. F.; Aiken, A. C.; Sueper, D.; Jimenez, J. L.; Martin, S. T. Loading-Dependent Elemental Composition of α-Pinene SOA Particles. *Atmos. Chem. Phys.* **2009**, *9* (3), 771−782.
(51) Kobayashi, S.; Higashimura, H. Oxidative Polymerization of Phenols Revisited. *Prog. Polym. Sci.* **2003**, *28* (6), 1015−1048.
(52) Braga, D.; Christophis, C.; Noll, S.; Hampp, N. Selective Photochemical Synthesis of 3,3′-Dimethoxy-4,2′-Dihydroxybiphenyl. *J. Photochem. Photobiol. A Chem.* **2005**, *172* (2), 115−120.
(53) McLafferty, F. W. *Mass Spectral Correlations*; In Advances in Chemistry Series; American Chemical Society, 1963.
(54) Jiang, W.; Misovich, M. V.; Hettiyadura, A. P. S.; Laskin, A.; McFall, A. S.; Anastasio, C.; Zhang, Q. Photosensitized Reactions of a Phenolic Carbonyl from Wood Combustion in the Aqueous Phase—Chemical Evolution and Light Absorption Properties of AqSOA. *Environ. Sci. Technol.* **2021**, *55* (8), 5199−5211.
(55) Jiang, W.; Niedek, C.; Anastasio, C.; Zhang, Q. Photoaging of Phenolic Secondary Organic Aerosol in the Aqueous Phase: Evolution of Chemical and Optical Properties and Effects of Oxidants. *Atmos. Chem. Phys.* **2023**, *23* (12), 7103−7120.
(56) Farley, R. N.; Collier, S.; Cappa, C. D.; Williams, L. R.; Onasch, T. B.; Russell, L. M.; Kim, H.; Zhang, Q. Source Apportionment of Soot Particles and Aqueous-Phase Processing of Black Carbon Coatings in an Urban Environment. *Atmos. Chem. Phys.* **2023**, *23* (23), 15039−15056.
(57) Takegawa, N.; Miyakawa, T.; Kawamura, K.; Kondo, Y. Contribution of Selected Dicarboxylic and ω-Oxocarboxylic Acids in Ambient Aerosol to the m/z 44 Signal of an Aerodyne Aerosol Mass Spectrometer. *Aerosol Sci. Technol.* **2007**, *41* (4), 418−437.
(58) Sorooshian, A.; Murphy, S. M.; Hersey, S.; Bahreini, R.; Jonsson, H.; Flagan, R. C.; Seinfeld, J. H. Constraining the Contribution of Organic Acids and AMS m/z 44 to the Organic Aerosol Budget: On the Importance of Meteorology, Aerosol Hygroscopicity, and Region. *Geophys. Res. Lett.* **2010**, *37*(21) L21807. .
(59) Duplissy, J.; DeCarlo, P. F.; Dommen, J.; Alfarra, M. R.; Metzger, A.; Barmpadimos, I.; Prevot, A. S. H.; Weingartner, E.; Tritscher, T.; Gysel, M.; Aiken, A. C.; Jimenez, J. L.; Canagaratna, M. R.; Worsnop, D. R.; Collins, D. R.; Tomlinson, J.; Baltensperger, U. Relating Hygroscopicity and Composition of Organic Aerosol Particulate Matter. *Atmos. Chem. Phys.* **2011**, *11* (3), 1155−1165.
(60) Canagaratna, M. R.; Jimenez, J. L.; Kroll, J. H.; Chen, Q.; Kessler, S. H.; Massoli, P.; Hildebrandt Ruiz, L.; Fortner, E.; Williams, L. R.; Wilson, K. R.; Surratt, J. D.; Donahue, N. M.; Jayne, J. T.; Worsnop, D. R. Elemental Ratio Measurements of Organic Compounds Using Aerosol Mass Spectrometry: Characterization, Improved Calibration, and Implications. *Atmos. Chem. Phys.* **2015**, *15* (1), 253−272.
(61) Alfarra, M. R.; Coe, H.; Allan, J. D.; Bower, K. N.; Boudries, H.; Canagaratna, M. R.; Jimenez, J. L.; Jayne, J. T.; Garforth, A. A.; Li, S.-M.; Worsnop, D. R. Characterization of Urban and Rural Organic Particulate in the Lower Fraser Valley Using Two Aerodyne Aerosol Mass Spectrometers. *Atmos. Environ.* **2004**, *38* (34), 5745−5758.
(62) Aiken, A. C.; DeCarlo, P. F.; Jimenez, J. L. Elemental Analysis of Organic Species with Electron Ionization High-Resolution Mass Spectrometry. *Anal. Chem.* **2007**, *79* (21), 8350−8358.
(63) Pieber, S. M.; El Haddad, I.; Slowik, J. G.; Canagaratna, M. R.; Jayne, J. T.; Platt, S. M.; Bozzetti, C.; Daellenbach, K. R.; Fröhlich, R.; Vlachou, A.; Klein, F.; Dommen, J.; Miljevic, B.; Jiménez, J. L.; Worsnop, D. R.; Baltensperger, U.; Prévôt, A. S. H. Inorganic Salt Interference on CO2+ in Aerodyne AMS and ACSM Organic Aerosol Composition Studies. *Environ. Sci. Technol.* **2016**, *50* (19), 10494−10503.
(64) Finewax, Z.; de Gouw, J. A.; Ziemann, P. J. Identification and Quantification of 4-Nitrocatechol Formed from OH and NO3 Radical-Initiated Reactions of Catechol in Air in the Presence of NOx: Implications for Secondary Organic Aerosol Formation from Biomass Burning. *Environ. Sci. Technol.* **2018**, *52* (4), 1981−1989.
(65) Hems, R. F.; Abbatt, J. P. D. Aqueous Phase Photo-Oxidation of Brown Carbon Nitrophenols: Reaction Kinetics, Mechanism, and Evolution of Light Absorption. *ACS Earth Sp. Chem.* **2018**, *2* (3), 225−234.
(66) Zhao, R.; Lee, A. K. Y.; Huang, L.; Li, X.; Yang, F.; Abbatt, J. P. D. Photochemical Processing of Aqueous Atmospheric Brown Carbon. *Atmos. Chem. Phys.* **2015**, *15* (11), 6087−6100.
(67) Levin, E. J. T.; Prenni, A. J.; Palm, B. B.; Day, D. A.; Campuzano-Jost, P.; Winkler, P. M.; Kreidenweis, S. M.; DeMott, P. J.; Jimenez, J. L.; Smith, J. N. Size-Resolved Aerosol Composition and Its Link to Hygroscopicity at a Forested Site in Colorado. *Atmos. Chem. Phys.* **2014**, *14* (5), 2657−2667.
(68) Fisseha, R.; Dommen, J.; Sax, M.; Paulsen, D.; Kalberer, M.; Maurer, R.; Höfler, F.; Weingartner, E.; Baltensperger, U.; Ho, F. Identification of Organic Acids in Secondary Organic Aerosol and the Corresponding Gas Phase from Chamber Experiments. *Anal. Chem.* **2004**, *76* (22), 6535−6540.
(69) Carlton, A. G.; Turpin, B. J.; Altieri, K. E.; Seitzinger, S.; Reff, A.; Lim, H.-J.; Ervens, B. Atmospheric Oxalic Acid and SOA Production from Glyoxal: Results of Aqueous Photooxidation Experiments. *Atmos. Environ.* **2007**, *41* (35), 7588−7602.
(70) Dong, P.; Chen, Z.; Qin, X.; Gong, Y. Water Significantly Changes the Ring-Cleavage Process During Aqueous Photooxidation of Toluene. *Environ. Sci. Technol.* **2021**, *55* (24), 16316−16325.
(71) Faust, J. A.; Wong, J. P. S.; Lee, A. K. Y.; Abbatt, J. P. D. Role of Aerosol Liquid Water in Secondary Organic Aerosol Formation from Volatile Organic Compounds. *Environ. Sci. Technol.* **2017**, *51* (3), 1405−1413.
(72) Andino, J. M.; Smith, J. N.; Flagan, R. C.; Goddard, W. A.; Seinfeld, J. H. Mechanism of Atmospheric Photooxidation of Aromatics: A Theoretical Study. *J. Phys. Chem.* **1996**, *100* (26), 10967−10980.
(73) Clark, J.; English, A. M.; Hansen, J. C.; Francisco, J. S. Computational Study on the Existence of Organic Peroxy Radical-Water Complexes (RO2·H2O). *J. Phys. Chem. A* **2008**, *112* (7), 1587−1595.
(74) Schuchmann, M. N.; Von Sonntag, C. The Rapid Hydration of the Acetyl Radical. A Pulse Radiolysis Study of Acetaldehyde in Aqueous Solution. *J. Am. Chem. Soc.* **1988**, *110* (17), 5698−5701.
(75) Ng, N. L.; Canagaratna, M. R.; Zhang, Q.; Jimenez, J. L.; Tian, J.; Ulbrich, I. M.; Kroll, J. H.; Docherty, K. S.; Chhabra, P. S.; Bahreini, R.; Murphy, S. M.; Seinfeld, J. H.; Hildebrandt, L.; Donahue, N. M.; DeCarlo, P. F.; Lanz, V. A.; Prévôt, A. S. H.; Dinar, E.; Rudich, Y.; Worsnop, D. R. Organic Aerosol Components

https://doi.org/10.1021/acsearthspacechem.4c00204
ACS Earth Space Chem. 2024, 8, 2270−2283

Observed in Northern Hemispheric Datasets from Aerosol Mass Spectrometry. *Atmos. Chem. Phys.* **2010**, *10* (10), 4625−4641.
(76) Schneider, J.; Weimer, S.; Drewnick, F.; Borrmann, S.; Helas, G.; Gwaze, P.; Schmid, O.; Andreae, M. O.; Kirchner, U. Mass Spectrometric Analysis and Aerodynamic Properties of Various Types of Combustion-Related Aerosol Particles. *Int. J. Mass Spectrom.* **2006**, *258* (1), 37−49.
(77) Hu, W. W.; Campuzano-Jost, P.; Palm, B. B.; Day, D. A.; Ortega, A. M.; Hayes, P. L.; Krechmer, J. E.; Chen, Q.; Kuwata, M.; Liu, Y. J.; de Sá, S. S.; McKinney, K.; Martin, S. T.; Hu, M.; Budisulistiorini, S. H.; Riva, M.; Surratt, J. D.; St. Clair, J. M.; Isaacman-Van Wertz, G.; Yee, L. D.; Goldstein, A. H.; Carbone, S.; Brito, J.; Artaxo, P.; de Gouw, J. A.; Koss, A.; Wisthaler, A.; Mikoviny, T.; Karl, T.; Kaser, L.; Jud, W.; Hansel, A.; Docherty, K. S.; Alexander, M. L.; Robinson, N. H.; Coe, H.; Allan, J. D.; Canagaratna, M. R.; Paulot, F.; Jimenez, J. L. Characterization of a Real-Time Tracer for Isoprene Epoxydiols-Derived Secondary Organic Aerosol (IEPOX-SOA) from Aerosol Mass Spectrometer Measurements. *Atmos. Chem. Phys.* **2015**, *15* (20), 11807−11833.
(78) Cubison, M. J.; Ortega, A. M.; Hayes, P. L.; Farmer, D. K.; Day, D.; Lechner, M. J.; Brune, W. H.; Apel, E.; Diskin, G. S.; Fisher, J. A.; Fuelberg, H. E.; Hecobian, A.; Knapp, D. J.; Mikoviny, T.; Riemer, D.; Sachse, G. W.; Sessions, W.; Weber, R. J.; Weinheimer, A. J.; Wisthaler, A.; Jimenez, J. L. Effects of Aging on Organic Aerosol from Open Biomass Burning Smoke in Aircraft and Laboratory Studies. *Atmos. Chem. Phys.* **2011**, *11* (23), 12049−12064.
(79) Ng, N. L.; Canagaratna, M. R.; Jimenez, J. L.; Zhang, Q.; Ulbrich, I. M.; Worsnop, D. R. Real-Time Methods for Estimating Organic Component Mass Concentrations from Aerosol Mass Spectrometer Data. *Environ. Sci. Technol.* **2011**, *45* (3), 910−916.
(80) Zhang, Q.; Alfarra, M. R.; Worsnop, D. R.; Allan, J. D.; Coe, H.; Canagaratna, M. R.; Jimenez, J. L. Deconvolution and Quantification of Hydrocarbon-like and Oxygenated Organic Aerosols Based on Aerosol Mass Spectrometry. *Environ. Sci. Technol.* **2005**, *39* (13), 4938−4952.
(81) Hinks, M. L.; Montoya-Aguilera, J.; Ellison, L.; Lin, P.; Laskin, A.; Laskin, J.; Shiraiwa, M.; Dabdub, D.; Nizkorodov, S. A. Effect of Relative Humidity on the Composition of Secondary Organic Aerosol from the Oxidation of Toluene. *Atmos. Chem. Phys.* **2018**, *18* (3), 1643−1652.
(82) Vöhringer-Martinez, E.; Hansmann, B.; Hernandez, H.; Francisco, J. S.; Troe, J.; Abel, B. Water Catalysis of a Radical-Molecule Gas-Phase Reaction. *Science* **2007**, *315* (5811), 497−501.

https://doi.org/10.1021/acsearthspacechem.4c00204
ACS Earth Space Chem. 2024, 8, 2270−2283